

A Li-ion battery charger based on LDO regulator with pre-charge mode in 180 nm CMOS technology

Mounir Ouremchi¹, Karim El Khadiri², Hassan Qjidaa¹, Mohammed Ouazzani Jamil³

¹Department of Physics, Faculty of Sciences, Sidi Mohamed Ben Abdellah University, Fez, Morocco

²Laboratory of Computer Science and Interdisciplinary Physics, Normal Superior School,
Sidi Mohamed Ben Abdellah University, Fez, Morocco

³Department of Physics, Private University of Fez, Fez, Morocco

Article Info

Article history:

Received Feb 21, 2023

Revised Jun 8, 2023

Accepted Jun 25, 2023

Keywords:

Constant current mode

Constant voltage mode

Control modes

Fast constant current mode

LDO regulator

Li-ion battery charging process

Pre-charge current mode

ABSTRACT

This paper presents a novel Li-ion battery charger that utilizes a low-dropout (LDO) regulator and incorporates four control modes: low constant current mode, pre-charge current mode, fast constant current mode, and constant voltage mode. The charger aims to meet specific criteria such as high precision, high efficiency, and small form factor. Through simulation results, the following specifications were obtained using a 1.8 V supply in a 0.18 μm complementary metal–oxide–semiconductor (CMOS) technology: a trickle current of 124.7 mA, a pre-charge current of 466.94 mA, a maximum charge current of 1.06 A, and a charge voltage of 4.21 V. The proposed charger demonstrates an efficiency of 92%.

This is an open access article under the [CC BY-SA](https://creativecommons.org/licenses/by-sa/4.0/) license.



Corresponding Author:

Mounir Ouremchi

Department of Physics, Faculty of Sciences, Sidi Mohamed Ben Abdellah University

Fez, Morocco

Email: mounir.ouremchi@gmail.com

1. INTRODUCTION

Due to their compact size, light weight, and charging capabilities [1], wearable devices have become increasingly popular as high-tech products. Lithium-ion batteries are the favored option for these devices because they offer several advantages compared to other battery technologies. Among the advantages of lithium-ion batteries are their high energy density, minimal maintenance needs, elevated voltage output, absence of memory effect, and a diverse range of available types. However, the durability of lithium-ion batteries is contingent not just on the duration of charging but also on the effectiveness of overcharge control and charging strategies [2]. The constant current-constant voltage (CC-CV) technique is widely employed as the primary charging method for these batteries. This method combines constant current (CC) and constant voltage (CV) modes to effectively control the charging current and avoid the risk of overcharging [3]–[5].

In the literature, various battery charger architectures have been proposed, employing different power control methods to regulate the supply voltage. While some architectures, such as DC/DC converters or switched-mode power supplies, offer high efficiency [1], [6]–[8], these components are not appropriate for integration into a single chip, as well as may sacrifice accuracy for efficiency. Charge pumps have been utilized as adaptive supply voltages [3], but they suffer from significant current ripple and low efficiency. On the other hand, LDO-based (low-dropout) chargers exhibit low current ripple and can be integrated into chips without additional components [9], although their efficiency is often compromised. In this study, we enhance the efficiency of LDO-based chargers by incorporating a power transistor as a variable current source and

minimizing failure. One notable aspect missing in certain papers [1], [3], [6], [8]–[12] is temperature control during charging and the inclusion of trickle charge mode for fully discharged batteries [1], [13]. By introducing the fourth mode, known as pre-charge, the proposed integrated circuit serves as a comprehensive battery charger, encompassing all necessary charging and battery protection functions.

This document presents the design and simulation outcomes of the integrated battery charger that has been proposed. The charger employs a four-mode control system specifically designed for lithium-ion batteries, accommodating charging currents spanning from 124 mA to 1.6 A. In section 2, the conventional charging approach for lithium-ion batteries is explained, followed by section 3 which details the structure and operation of the essential components within the proposed integrated circuit. Simulation results are outlined in section 4, and section 5 concludes the paper.

2. LI-ION BATTERY CHARGING METHOD

Ensuring charging safety is a crucial requirement for Li-ion battery chargers. However, there exist certain restrictions on charging current and voltage. Consequently, the battery temperature experiences a rapid increase, leading to significant issues caused by these limitations. Interestingly, a battery can be fully charged within just one hour using a standard charging current of 1C [14]. To fulfill this objective, a typical lithium-ion battery charging profile depicted in Figure 1, encompasses three fundamental modes: trickle constant current, fast constant current, and constant voltage modes. Although, the conventional charging process may pose safety risks during the transition from low current to higher current levels, potentially causing damage to both the battery cell and the chip.

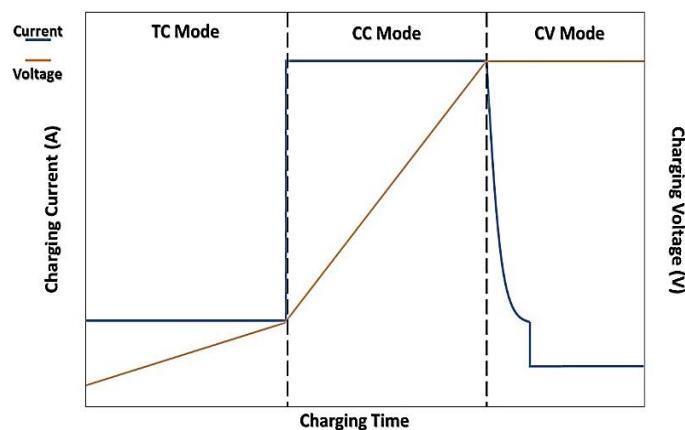


Figure 1. Typical charging process of a Li-ion battery

In this paper, a unique charging protocol is presented, introducing a novel fourth mode called the pre-charge mode alongside the conventional three modes, as illustrated in Figure 2. The primary objective of incorporating this innovative mode is to enhance the safety and reliability of the battery charging process, underlining its pivotal role in achieving these critical aspects. In the trickle constant current mode, when the battery voltage (V_{bat}) falls below 2.4 V, the internal resistance of the Li-ion battery increases. To address this, the charging process includes a trickle constant current phase, often referred to as the "overnight charger" [15]. Moving on to the pre-charge phase, when the V_{bat} exceeds 2.4 V, the process transitions from the first mode to the second mode. As the battery voltage ranges between 2.8 V and 4.2 V, the charging process enters the third mode known as the fast-constant current mode. Finally, when the battery voltage surpasses 4.2 V while the charger is in constant voltage mode, it switches to using a constant voltage to continue charging the battery. There are two methods for ending the charging process. The initial approach involves monitoring the minimum charge current during the constant voltage (CV) phase. Termination of the charging process occurs when the charging current descends outside the predetermined range, the second method, on the other hand, depends on observing a maximum charging duration [16].

Our chosen approach in the proposed design is to employ the first method for terminating the charging process. The battery will continue charging until the charging current decreases to or falls below $1C/40$. A visual representation of the entire charging process for our Li-ion battery charger is provided in Figure 3.

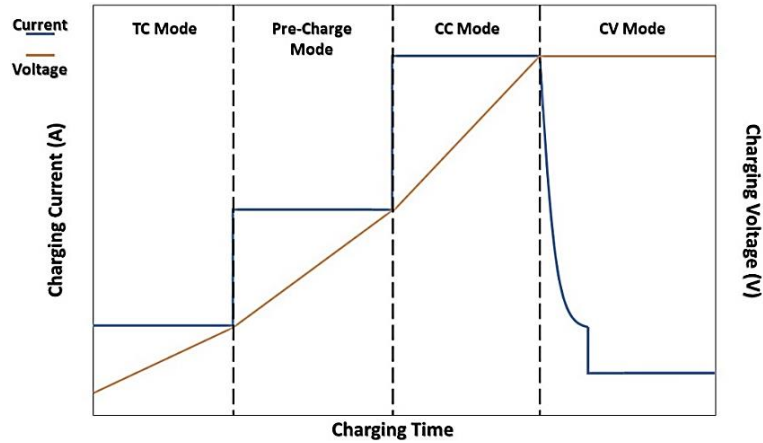


Figure 2. Proposed Li-ion battery charging process with pre-charge mode

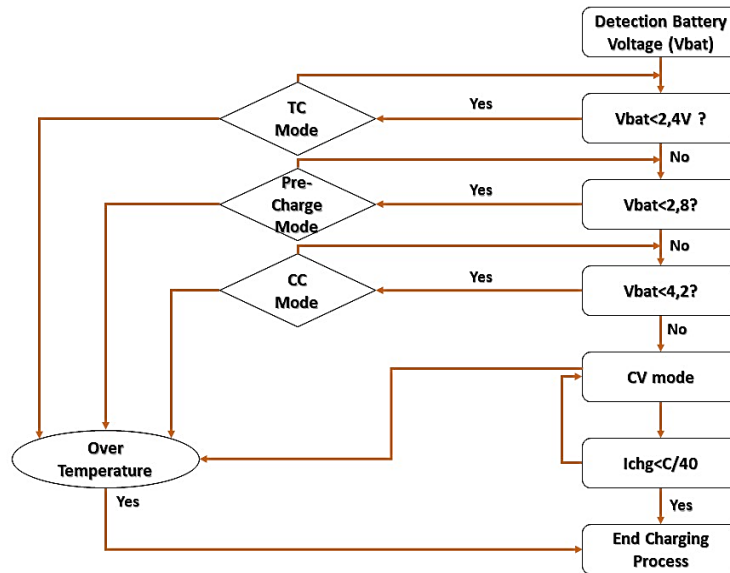


Figure 3. Battery charging with four modes flow chart

3. ARCHITECTURE DESCRIPTION

In contrast to other architectures that rely on a microprocessor for controlling different charging modes, our proposed architecture combines lithium-ion battery charging, float current, fast constant current, and constant voltage functionalities into a unified system, as depicted in Figure 4. The Analog module supports all three modes and encompasses several blocks, including the low dropout (LDO) regulator, current generator, current sense, and temperature sense (PTAT circuit). These components work together harmoniously to facilitate the charging process and ensure optimal performance.

To regulate the supply voltage, an LDO regulator is employed to generate V_{adapt} . The power transistor MP functions as a variable current source, a technique previously utilized in conjunction with a fly-back converter [10]. The MP control is achieved through the combined effects of three current sources, I_{ref1} , I_{ref2} , and I_{ref3} , generated by the current generator. These currents pass through a level shifter to ensure that transistor MP draws a consistent current of 124.7 mA, 466.94 mA, and 1.06 A during the TC, pre-charge, and CC modes respectively. In the CV mode, an integrator is employed for control purposes. An amplifier within the modes controller is utilized to halt the charging process under two conditions: the charging process concludes either when the battery reaches full capacity or when the temperature detected by the PTAT circuit surpasses 115 degrees.

The detailed structure of our proposed lithium-ion battery charger is depicted in Figure 5. An important feature of this architecture is the incorporation of current as a command parameter to regulate the switching of the power transistor MP, enabling it to function effectively as a variable current source. Three

reference currents namely I_{ref1} , I_{ref2} , and I_{ref3} are generated by the current generator and duplicated by current mirrors (M4 and M3). These currents are then applied to adjust the gate voltage of MP through level shifters.

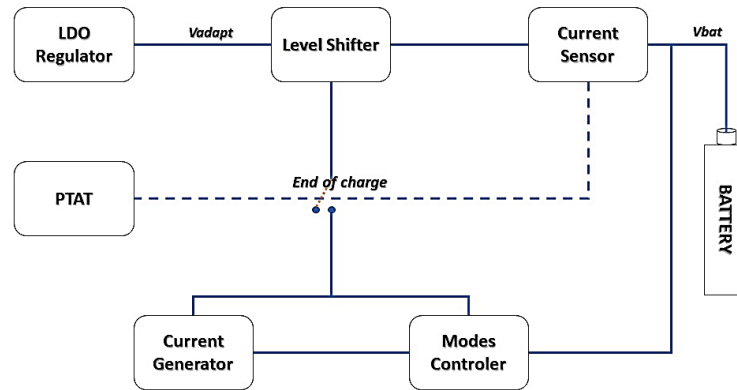


Figure 4. Simplified diagram of the proposed Li-ion battery charger

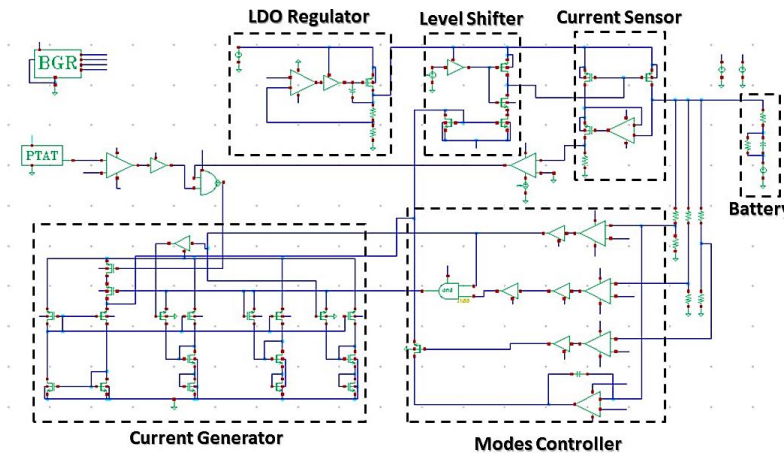


Figure 5. The proposed charger architecture

In contrast to the three current modes (TC, pre-charge, CC), the CV mode is governed by an integrator, following the principles outlined in [10]. As the voltage V_{fb1} gradually increases, the output of the integrator decreases, causing MP to act as a current sink until the charging process is terminated. A voltage-to-current converter can be employed to generate the CV current. Charging is considered complete when the current sensor detects that the charging current (I_{chg}) equals 20 mA, or when the die temperature exceeds 115 °C, leading to the deactivation of the PMOS (Meoc) integrated into the current generator. This occurrence happens sporadically to ensure the safety of the charging process.

3.1. LDO regulator

Figure 6 depicts the LDO regulator circuit employed in this architecture [17], [18]. The input reference voltage, V_{ref} , can be sourced from an error amplifier, power transistor, feedback resistor network, or a bandgap reference circuit (BGR). The power transistor performs a distinct function in the circuit. The load current and resistors R_{f1} and R_{f2} together form a feedback network within the LDO regulator. To facilitate high load currents and minimize dropout voltages, LDO regulators necessitate the use of large power transistors (MP). These transistors are capable of handling significant current levels and help maintain stable voltage regulation even under demanding load conditions. By incorporating such components, the LDO regulator can effectively provide a regulated and reliable supply voltage to the system.

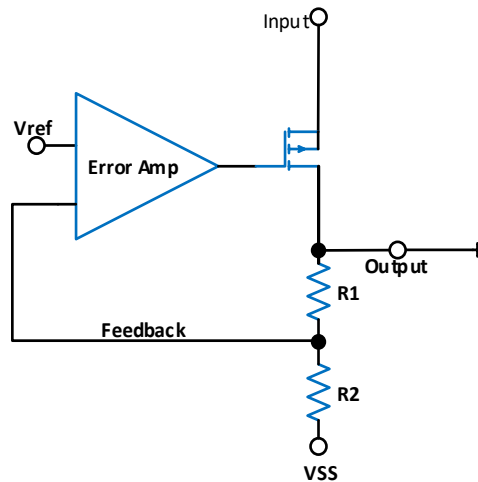


Figure 6. LDO regulator circuit design

Figure 7 illustrates the behavior of the LDO regulator, indicating that the output remains stable at 1.8 V. The output of the regulator is equal to or greater than the sum of the regulated voltage (nominal voltage) and the dropout voltage ($V_{in} = V_{out} + V_{do}$) when the input voltage (V_{in}) matches or exceeds this threshold. Conversely, if the input voltage (V_{in}) drops below the $V_{out} + V_{do}$ voltage threshold, the output of the regulator mirrors the input voltage. This means that the output voltage will decrease in response to a decrease in the input voltage. The dropout voltage (V_{do}) represents the minimum voltage difference required for the LDO regulator to maintain a stable output voltage. In this case, the system dropout is specified as 50.54 mV. It signifies that as long as the input voltage remains above the regulated voltage plus the dropout voltage, the LDO regulator will effectively maintain a stable output voltage of 1.8 V.

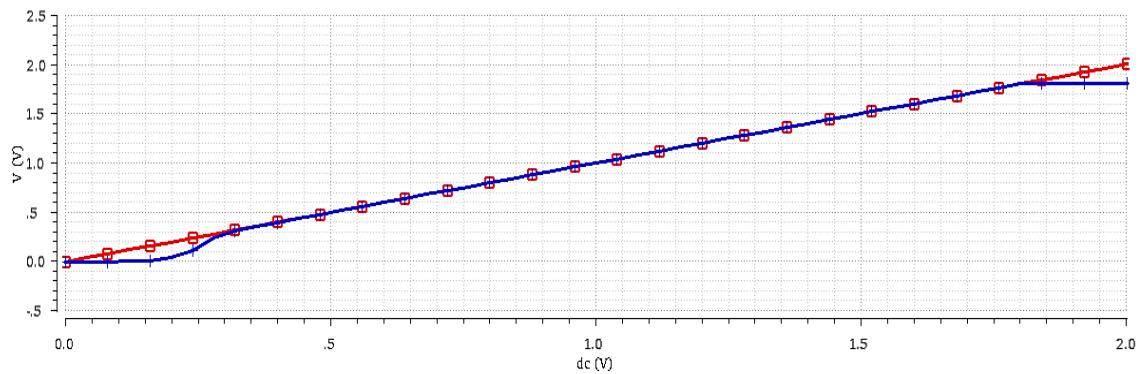


Figure 7. Simulation result of the LDO regulation curves

3.2. Current generator

The current generator in the architecture provides reference currents (I_{ref1} , I_{ref2} , and I_{ref3}) for controlling the TC, pre-charge, and CC modes. This architecture was chosen for its temperature insensitivity, as demonstrated in Figure 8. The circuit design of the current generator follows a conventional architecture (PM0-PM1-NM0-NM1) where the passive resistance is varied by the PMOS transistor PM3 the gate bias generator consists of two diode-connected NMOS transistors and one PMOS transistor, which are responsible for each mode. In the I_{ref1} mode, MN3, MN4, and PM4 are used, while NM6, NM7, and PM5 are employed in the I_{ref2} mode, and NM8, NM9, and PM6 are used in the I_{ref3} mode. By copying the reference current I , PM4 generates the gate voltage for PM3, resulting in the production of I_{ref1} . Through the control switches NM2, NM5, and NM10, the reference currents I_{ref1} , I_{ref2} , or I_{ref3} can be generated. The integration and cancellation transistor Meoc switcher are utilized to generate I_{ref1} , I_{ref2} , and I_{ref3} and to terminate the charging process.

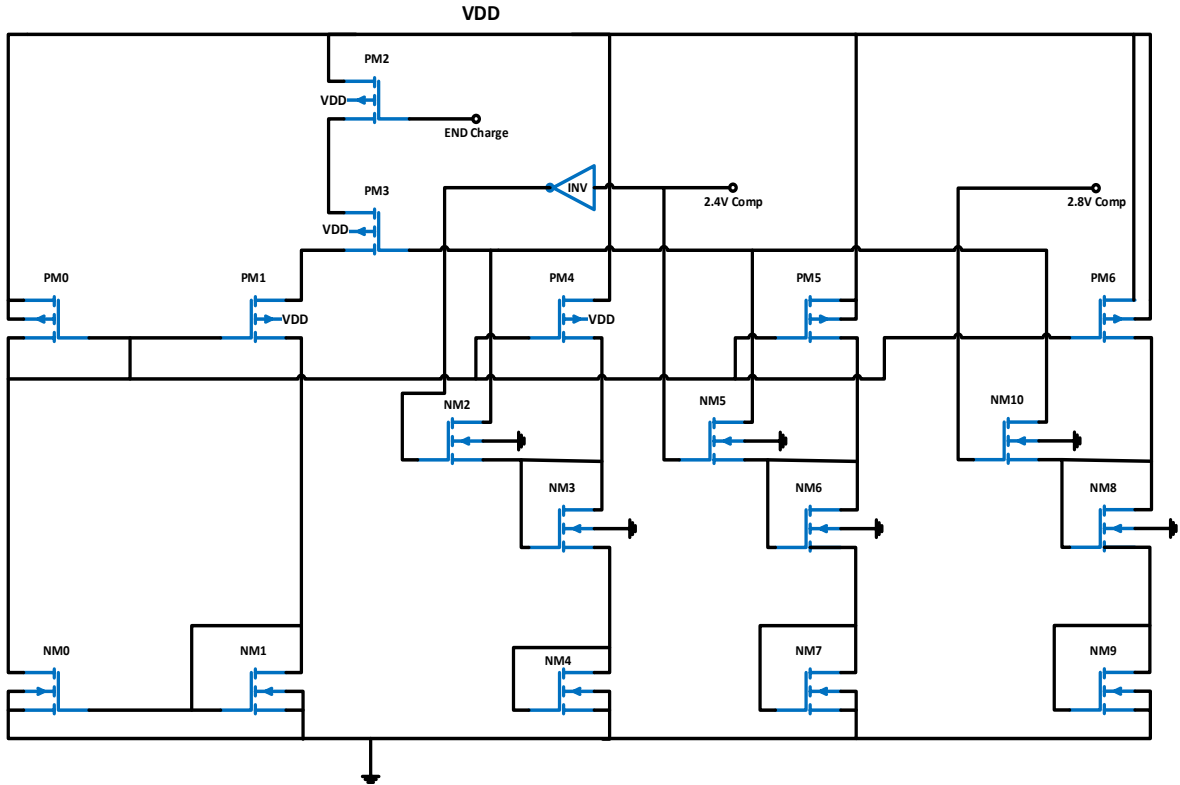


Figure 8. Current generator circuit design

3.3. Bandgap Reference Multioutput

The proposed design necessitates the use of four voltage references (V_{ref1} , V_{ref2} , V_{ref3} , V_{ref4}) and employs a multi-output bandgap voltage reference. Figure 9 showcases a precision temperature-compensated CMOS bandgap reference [19]–[22]. To enhance its functionality, four external stages have been added to generate reference voltages: $V_{ref1} = 1.37$ V, $V_{ref2} = 511.89$ mV, $V_{ref3} = 1.41$ V, and $V_{ref4} = 993.3$ mV. The formulas for the two generated currents (1) that are proportionate to V_{EB} and ΔV_{EB} , and bias the four additional stages, are as (1).

$$I_1 = I_2 = \alpha I_{ref1} = \beta I_{ref2} = \gamma I_{ref3} = \delta I_{ref4} \quad (1)$$

As illustrated in Figure 9, the current is split into two separate currents that flow through two branches, each consisting of a resistor and a bipolar transistor so that (2):

$$I_{11} = I_{22}; I_{12} = I_{21} \quad (2)$$

We have taken $R_2 = R_3$, to make the voltage at point A equal to the voltage at point B. The inputs of the amplifier are identical. As a result, the reference voltage for the proposed multi-output Bandgap reference (BGR) can be acquired from the output (3)-(6):

$$V_{ref1} = \frac{R_4}{\alpha} \left(\frac{\Delta V_{EB}}{R_1} + \frac{V_{EB1}}{R_2} \right) \quad (3)$$

$$V_{ref2} = \frac{R_5}{\beta} \left(\frac{\Delta V_{EB}}{R_1} + \frac{V_{EB1}}{R_2} \right) \quad (4)$$

$$V_{ref3} = \frac{R_6}{\gamma} \left(\frac{\Delta V_{EB}}{R_1} + \frac{V_{EB1}}{R_2} \right) \quad (5)$$

$$V_{ref4} = \frac{R_7}{\delta} \left(\frac{\Delta V_{EB}}{R_1} + \frac{V_{EB1}}{R_2} \right) \quad (6)$$

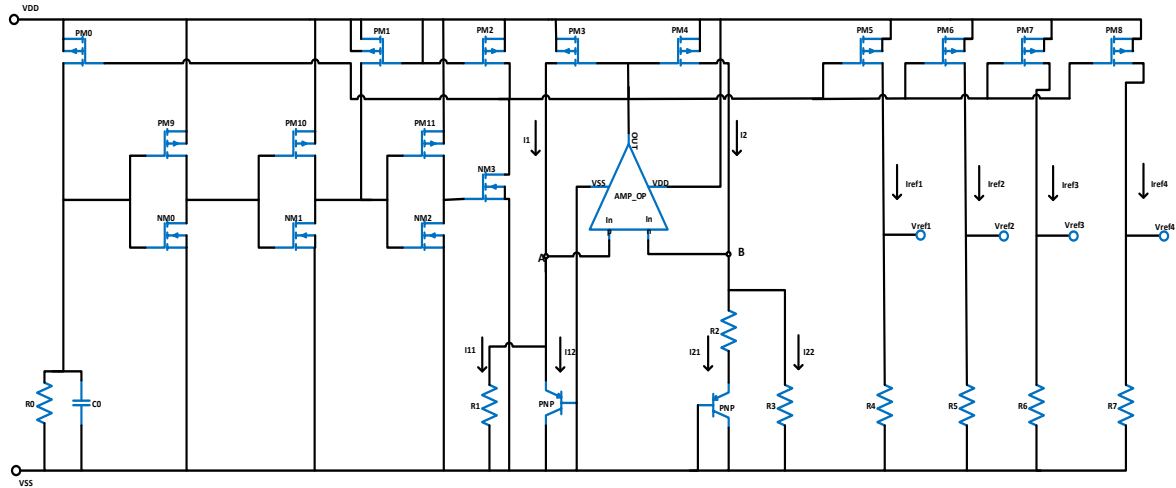


Figure 9. Bandgap reference multioutput circuit design

Figure 10 displays the simulation results of the reference voltages as a function of time. The obtained results demonstrate the stability of the reference voltages over time, with the following values: $V_{ref1} = 1.38\text{ V}$, $V_{ref2} = 0.511\text{ V}$, $V_{ref3} = 1.41\text{ V}$, and $V_{ref4} = 1\text{ V}$. These values remain consistent and do not exhibit significant variations as time progresses.

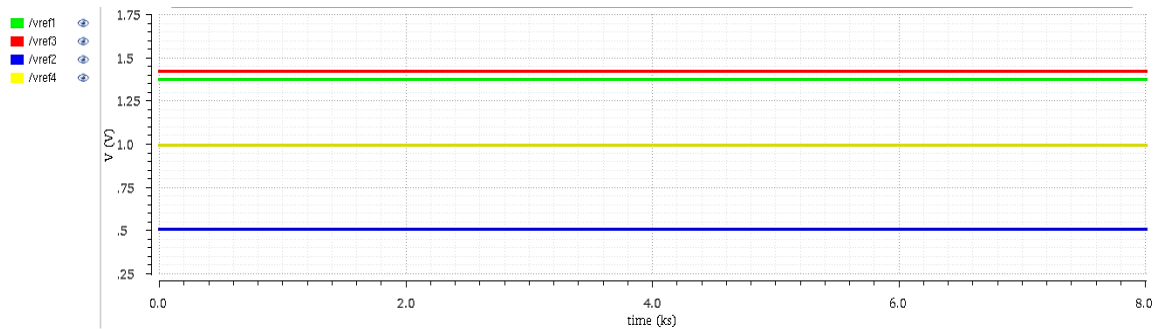


Figure 10. Simulation result of the bandgap outputs with time variation

In Figure 11, the behavior of the reference voltages as a function of temperature is presented, covering a range from $-150\text{ }^{\circ}\text{C}$ to $150\text{ }^{\circ}\text{C}$. The simulation results confirm that the reference voltages remain independent of temperature, with the approximate values: $V_{ref1} \approx 1.37\text{ V}$, $V_{ref2} \approx 0.52\text{ V}$, $V_{ref3} \approx 1.42\text{ V}$, and $V_{ref4} \approx 994.3\text{ mV}$. These results demonstrate the robust temperature compensation capability of the design, ensuring that the reference voltages remain stable and unaffected by temperature fluctuations within the specified temperature range.

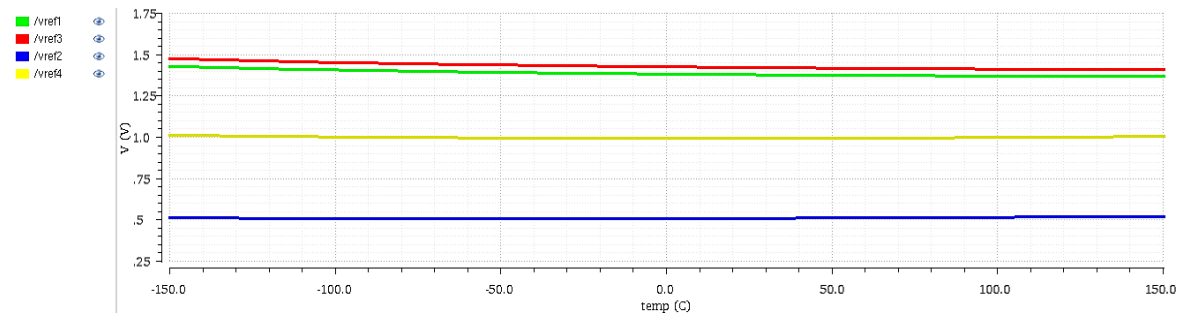


Figure 11. Simulation result of bandgap outputs with temperature variation

3.4. Current sensor

Utilizing the current sensor transistor or M_{cs} in the depicted current sensing circuit, as illustrated in Figure 12, enabled the accurate detection of electrical current passing through the power transistor MP. This deliberate design decision was implemented to ensure a harmonious relationship between the voltages of M_{cs} and voltage source drain (V_{sd}) of MP, emphasizing the importance of a balanced configuration for optimal performance.

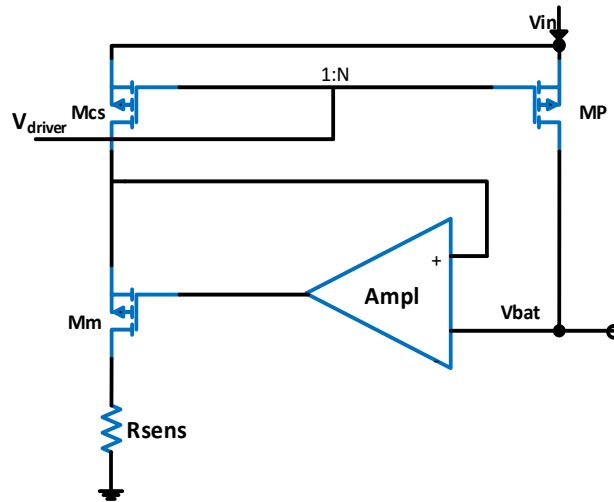


Figure 12. Current sensor circuit design

4. SIMULATION RESULTS AND DISCUSSION

Implementation, testing, and design of the proposed architecture were accomplished using CADENCE Virtuoso and 180 nm CMOS technology. The simulation results, depicted in Figure 13, exhibit the sensing currents' waveforms, including both charge current (I_{chg}) and sense current (I_{sens}), organized from top to bottom. The behavior and performance of the architecture during operation are illuminated by these waveforms. The charge current waveform illustrates the current entering the battery during the charging process, and the sense current waveform signifies the current detected by the current sensing circuitry. Analyzing these waveforms can help assess the accuracy and efficiency of the charging process, ensuring that the current sensing mechanism is functioning as intended. These simulation results play a crucial role in evaluating the performance and reliability of the proposed architecture in practical scenarios.

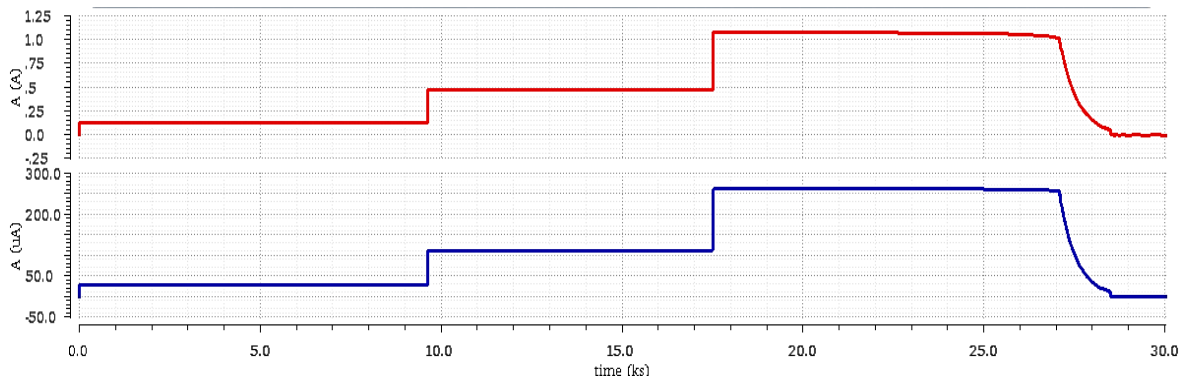


Figure 13. Simulation result of I_{sens} (blue) and I_{chg} (red)

Figure 14 presents the simulated waveform results for the proposed Li-ion battery charger. The waveform depicts the behavior of the charger during different charging modes. The reference currents used in

the simulation are 124.4 mA, 466.94 mA, and 1.06 A for the float, precharge, and fast constant current modes, respectively. The voltage ranges for these modes are defined as 2.4 V and 4.2 V.

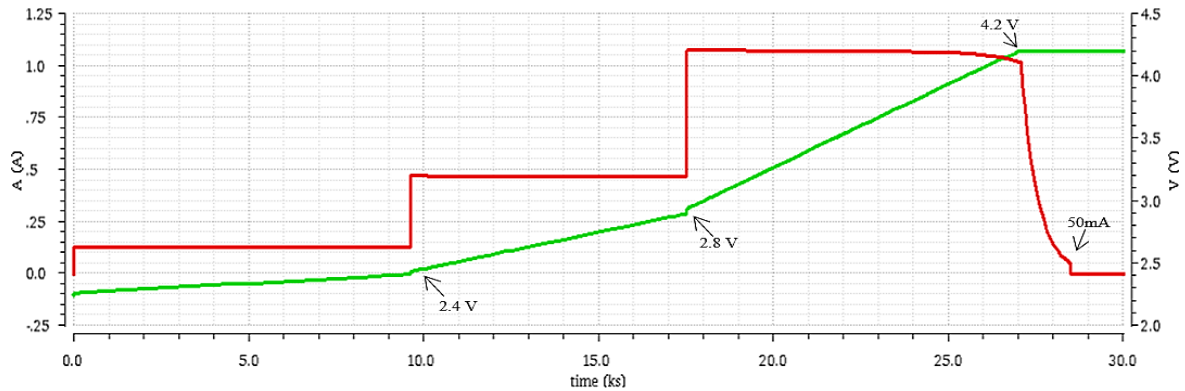


Figure 14. Simulation results of the proposed Li-ion battery charger

The stopping current, which indicates the point at which charging is terminated, is set to 50 mA. This corresponds to approximately 1C/40, as per the defined charging parameters. The efficiency of the system, depicted in Figure 15, varies with the output power. Simulation results reveal a peak efficiency of 92% in the proposed system. This outcome underscores the effectiveness and energy efficiency of the implemented power management approach. Table 1 offers a comparative analysis of the proposed power management system and previous works, presenting a summary of key features and performance metrics from various approaches. This facilitates an evaluation of the advantages and progressions provided by the proposed architecture in contrast to existing solutions.

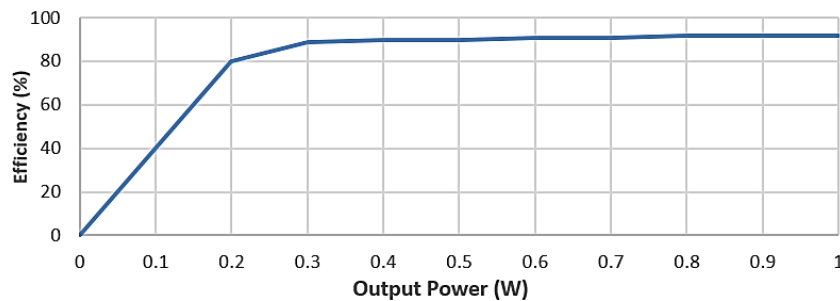


Figure 15. Proposed circuit efficiency versus output power

Table 1. Summary and comparison performances

Reference	Ziadi and Qjidaa [21]	Jung <i>et al.</i> [23]	Chung <i>et al.</i> [24]	Farah <i>et al.</i> [25]	This Work
CMOS process	180 nm	180 nm	130 nm BICMOS	180 nm	180 nm
Topology	LDO Reg	Switching based and LDO Reg	LDO Reg	LDO Reg	LDO Reg
Output voltage	2.8-4.2 V	2.8-4.2 V	3-4.3 V	2.8-4.2 V	2.4-4.2 V
Maximum charging current	448 mA	500 mA	495 mA	1A	1.06 A
Efficiency	87%	87.6%	83.9%	90.9%	92%

5. CONCLUSION




To summarize, a new integrated Li-ion battery charger has been developed based on an LDO regulator, incorporating four control modes: float constant current, pre-charge current, fast constant current, and constant voltage. The charger focuses on important criteria for lithium-ion chargers, such as high accuracy, high efficiency, and compact size. Through simulations, the proposed charger achieves a trickle current of 124.7 mA, a pre-charge current of 466.94 mA, a maximum charge current of 1.06 A, and a charge voltage of

4.21 V, all powered by a 1.8 V supply. The proposed system exhibits an estimated efficiency of 92% using 0.18 μm CMOS technology, meeting the desired objectives of the lithium-ion charger.




REFERENCES

- [1] D. Deng, "Li-ion batteries: Basics, progress, and challenges," *Energy Science and Engineering*, vol. 3, no. 5, pp. 385–418, Sep. 2015, doi: 10.1002/ese3.95.
- [2] D. Linden and T. B. Reddy, *Handbook of batteries*, 3rd ed., vol. 33, no. 04. McGraw-Hill Professional, 1995.
- [3] Y. S. Hwang, S. C. Wang, F. C. Yang, and J. J. Chen, "New compact CMOS li-ion battery charger using charge-pump technique for portable applications," *IEEE Transactions on Circuits and Systems I: Regular Papers*, vol. 54, no. 4, pp. 705–712, Apr. 2007, doi: 10.1109/TCSI.2007.890605.
- [4] J. Buxton, "Li-Ion battery charging requires accurate voltage sensing," *Analog Dialogue: Analog Devices*, vol. 31, no. 2, pp. 3–4, 1997.
- [5] C. H. Lin, C. Y. Hsieh, and K. H. Chen, "A Li-ion battery charger with smooth control circuit and built-in resistance compensator for achieving stable and fast charging," *IEEE Transactions on Circuits and Systems I: Regular Papers*, vol. 57, no. 2, pp. 506–517, Feb. 2010, doi: 10.1109/TCSI.2009.2023830.
- [6] H. Y. Yang, T. H. Wu, J. J. Chen, Y. S. Hwang, and C. C. Yu, "An omnipotent Li-Ion battery charger with multimode controlled techniques," in *Proceedings of the International Conference on Power Electronics and Drive Systems*, Apr. 2013, pp. 531–534, doi: 10.1109/PEDS.2013.6527076.
- [7] R. Pagano, M. Baker, and R. E. Radke, "A 0.18- μ monolithic li-ion battery charger for wireless devices based on partial current sensing and adaptive reference voltage," *IEEE Journal of Solid-State Circuits*, vol. 47, no. 6, pp. 1355–1368, Jun. 2012, doi: 10.1109/JSSC.2012.2191025.
- [8] F. C. Yang, C. C. Chen, J. J. Chen, Y. S. Hwang, and W. T. Lee, "Hysteresis-current-controlled buck converter suitable for Li-ion battery charger," in *2006 International Conference on Communications, Circuits and Systems, ICCAS, Proceedings*, Jun. 2006, vol. 4, pp. 2723–2726, doi: 10.1109/ICCCAS.2006.285232.
- [9] P. H. Van Quang, T. T. Ha, and J. W. Lee, "A fully integrated multimode wireless power charger IC with adaptive supply control and built-in resistance compensation," *IEEE Transactions on Industrial Electronics*, vol. 62, no. 2, pp. 1251–1261, Feb. 2015, doi: 10.1109/TIE.2014.2336618.
- [10] J. J. Chen, F. C. Yang, C. C. Lai, Y. S. Hwang, and R. G. Lee, "A high-efficiency multimode Li-Ion battery charger with variable current source and controlling previous-stage supply voltage," *IEEE Transactions on Industrial Electronics*, vol. 56, no. 7, pp. 2469–2478, Jul. 2009, doi: 10.1109/TIE.2009.2018435.
- [11] J. A. De Lima, "A compact and power-efficient CMOS battery charger for implantable devices," in *SBCCI 2014: Proceedings of the 27th Symposium on Integrated Circuits and Systems Design*, Sep. 2014, pp. 1–6, doi: 10.1145/2660540.2660988.
- [12] P. Li and R. Bashirullah, "A wireless power interface for rechargeable battery operated medical implants," *IEEE Transactions on Circuits and Systems II: Express Briefs*, vol. 54, no. 10, pp. 912–916, Oct. 2007, doi: 10.1109/TCSII.2007.901613.
- [13] S. H. Yang, J. W. Liu, and C. C. Wang, "A single-chip 60-V bulk charger for series Li-ion batteries with smooth charge-mode transition," *IEEE Transactions on Circuits and Systems I: Regular Papers*, vol. 59, no. 7, pp. 1588–1597, Jul. 2012, doi: 10.1109/TCSI.2011.2177137.
- [14] C. C. Tsai, C. Y. Lin, Y. S. Hwang, W. T. Lee, and T. Y. Lee, "A multi-mode LDO-based Li-ion battery charger in 0.35 μm CMOS technology," in *IEEE Asia-Pacific Conference on Circuits and Systems, Proceedings, APCCAS, 2004*, vol. 1, pp. 49–52, doi: 10.1109/apccas.2004.1412688.
- [15] R. C. Cope and Y. Podrazhansky, "The art of battery charging," in *Fourteenth Annual Battery Conference on Applications and Advances. Proceedings of the Conference (Cat. No.99TH8371)*, 1999, pp. 233–235, doi: 10.1109/BCAA.1999.795996.
- [16] S. Dearborn, "Charging Li-ion batteries for maximum run times," *Power Electronics Technology*, vol. 31, no. 4, pp. 40–49, 2005.
- [17] M. A. S. Bhuiyan *et al.*, "CMOS low-dropout voltage regulator design trends: an overview," *Electronics (Switzerland)*, vol. 11, no. 2, p. 193, Jan. 2022, doi: 10.3390/electronics11020193.
- [18] L. Sood and A. Agarwal, "A CMOS standard-cell based fully-synthesizable low-dropout regulator for ultra-low power applications," *AEU - International Journal of Electronics and Communications*, vol. 141, p. 153958, Nov. 2021, doi: 10.1016/j.aeue.2021.153958.
- [19] S. S. Bethi, K. S. Lee, R. Veillette, J. Carletta, and M. Willett, "A temperature and process insensitive CMOS reference current generator," in *Midwest Symposium on Circuits and Systems*, Aug. 2013, pp. 301–304, doi: 10.1109/MWSCAS.2013.6674645.
- [20] Abhisek Dey and T. K. Bhattacharyya, "Design of a CMOS Bandgap Reference with Low Temperature Coefficient and High Power Supply Rejection Performance," *International Journal of VLSI Design & Communication Systems*, vol. 2, no. 3, pp. 139–150, Sep. 2011, doi: 10.5121/vlsic.2011.2312.
- [21] Y. Ziadi and H. Qjidaa, "A high efficiency Li-ion battery LDO-based charger for portable application," *Active and Passive Electronic Components*, vol. 2015, pp. 1–9, 2015, doi: 10.1155/2015/591986.
- [22] M. Ourenchi *et al.*, "Li-ion battery charger based on LDO regulator for portable device power management," in *Proceedings of 2018 6th International Renewable and Sustainable Energy Conference, IRSEC 2018*, Dec. 2018, pp. 1–4, doi: 10.1109/IRSEC.2018.8702961.
- [23] Y. H. Jung, S. K. Hong, and O. K. Kwon, "Highly accurate and power-efficient battery charger with charging current compensator for wearable devices," *Electronics Letters*, vol. 53, no. 7, pp. 461–463, Mar. 2017, doi: 10.1049/el.2017.0388.
- [24] K. Chung, S. K. Hong, and O. K. Kwon, "A fast and compact charger for an Li-Ion battery using successive built-in resistance detection," *IEEE Transactions on Circuits and Systems II: Express Briefs*, vol. 64, no. 2, pp. 161–165, Feb. 2017, doi: 10.1109/TCSII.2016.2554839.
- [25] F. Farah *et al.*, "A new Li-ion battery charger with charge mode selection based on 0.18 μm CMOS for phone applications," *International Journal of Electrical and Computer Engineering (IJECE)*, vol. 11, no. 3, pp. 1994–2002, 2021, doi: 10.11591/ijece.v11i3.pp1994-2002.




BIOGRAPHIES OF AUTHORS

Mounir Ouremchi    received his Ph.D. degree in Electrical Engineering from Faculty of Sciences Dhar EL Mahraz, Fez, Morocco, in 2022. In 2018 he was a guest researcher at LIMA laboratory in UQO, Quebec, Canada His main research interest includes renewable energy, switch mode audio amplifier, CMOS mixed-mode integrated circuit design, design techniques for RFID, Signal and image analysis, Li-ion battery charger, power management, and bio-electronics bio-medical applications. He can be contacted at email: mounir.ouremchi@gmail.com.






Karim El Khadiri    is now a Professor in Superior Normal School, ENS-FEZ, Morocco. He received his Master degree since 2011 in Micro-Electronics and Ph.D. degrees since 2017 in FSDM, USMBA, Fez, Morocco. His research interests include Li-Ion battery charger interface (BCI) and BMS, RFID passive and active tags, CMOS mixed mode integrated circuit design, Integrated Class-D power output stage, and renewable energy. He can be contacted at email: karim.elkhadiri@usmba.ac.ma.



Hassan Qjidaa    is now a Professor in Department of Physics, FSDM, USMBA, Fez, Morocco. He received his Master degree since 1984 and Ph.D. degrees since 1987 in Electrical Engineering from Nuclear Physics Institute of Lyon, France. His research interests include Li-Ion battery charger interface (BCI) and BMS, RFID passive and active tags, CMOS mixed mode integrated circuit design, integrated class-D power output stage, renewable energy, and image processing. He can be contacted at email: qjidah@yahoo.fr.



Mohammed Ouazzani Jamil    is currently the Dean of the faculty of engineering sciences, and a Professor in Private university of Fez (UPF). He does research in Condensed Matter Physics, Hamiltonian system, chaos, renewable energy, and artificial intelligence. Their current project is dynamic systems. He can be contacted at email: Ouazzani@upf.ac.ma.